Theor Chim Acta (1987) 71: 411-423

Theoretica Chimica Acta

A CASSCF and CCI study of the formation of the $Ni_2(C_2H_4)$ complex

Per-Olof Widmark and Björn O. Roos

Department of Theoretical Chemistry, Chemical Centre, P.O.B. 124, S-221 00 Lund, Sweden

(Received August 20, 1986; revised and accepted March 5, 1987)

Complete active space SCF and contracted CI calculations have been performed on the potential surface of the Ni_2-C_2H_4 complex in the singlet state. The ethene geometry and position relative to Ni_2 was optimized while the Ni-Ni distance was kept fixed at 2.5 Å.

Four possible symmetric geometric arrangements were considered, yielding only an end on π-bonded structure as bound. This is a consequence of the charge buildup between the nickel atoms and charge depletion at the ends, coupled with electron mobility along the bond axis, in the nickel dimer.

The energy minimum corresponds to a C_2H_4 moiety distorted 21% towards a C_2H_6 geometry, with a bond energy o 24.6 kcal/mol at the CCI level and 28.1 kcal/mol with cluster corrections included. The binding is described by a donation backdonation mechanism. These results are discussed in connection with earlier work on $Ni(C_2H_4)$ and $Ni_2(C_2H_4)$ and in connection with experimental work.

Key words: Organometallic bonding — Ni-ethene complex — Bond strength — Structure — CASSCF-CI

1. Introduction

The transition metal olefin bond is of fundamental importance in organometallic chemistry, and understanding of the mechanisms involved in its formation is essential to the understanding of organometallic chemistry, which has many important areas of application, such as homogeneous and heterogeneous catalysis. Complexed olefins, for example, are used as starting agents in many types of

reactions in homogeneous catalysis [1]. Recent progress in experimental methods has enabled high precision work on isolated complexes consisting of small organic/inorganic molecules and small metal clusters, especially in the field of matrix isolation techniques [2] and molecular beams [3]. The development of *ab initio* quantum chemistry during the last five years has made it possible to predict the properties of small molecules containing transition metal atoms to a reasonable accuracy. A number of such studies have also been performed using current MCSCF and CI techniques (see for example Ref. [4–12]).

One important class of molecules which has been studied extensively is NiX, where X is a small molecule like CO, C_2H_4 or C_2H_2. These molecules were previously thought to be very weakly bound with a triplet ground state arising from the $d^9s(^3D)$ configuration of nickel [4, 5]. Rives and Fenske [6] showed, however, that NiCO had a singlet ground state. The bond energy has later been computed to be close to 30 kcal/mol [7, 8]. The binding occurs through a mixture of the $d^9s(^1D)$ and $d^{10}(^1S)$ configurations of nickel where the dominating feature is an *sd* hybridization, which unshields the nickel atom making room for a reasonably strong dative bond [7, 9]. The same bonding mechanism occurs for other NiX compounds [9, 10] and is also found in the corresponding low spin iron systems [8]. It is also responsible for the low barrier found in the reaction between singlet nickel and hydrogen [11] and for the chemisorption of hydrogen molecules to a nickel surface [12].

In a previous paper we have reported a detailed investigation of the bonding mechanism and electronic structure of NiC_2H_4 [9]. The present contribution presents the results from a corresponding study of the association of C_2H_4 to a nickel dimer. The ethene-nickel system has been chosen as a typical example describing the bonding between a small transition metal cluster and an organic molecule. Future studies will include also clusters with a larger number of nickel atoms.

Three earlier theoretical studies of $Ni_2(C_2H_4)$ have appeared in the literature [4, 5, 13]. The SCF-Xα calculation by Rösch and Rhodin [13] does not include a discussion of structures and total energy and is therefore of less interest in connection with the present work. Basch et al. [5] find in their SCF-CI study the "end on" π coordinated structure (cf Fig. 1a) to be more stable than the $d\sigma - Ni_2(C_2H_4)$ structure (Fig. 1b). The same result was obtained by Ozin et al. [4] in their GVB-CI calculation. They estimated the bond energy to be around 27 kcal/mol, assuming a $^3A_2$ ground state configuration. The geometry of the ethene moiety was found to be only slightly distorted compared to the free molecule ($\delta R_{CC} = 0.02$ Å and CH bonds bend 2° out of the ethene plane). These results are very similar to those found for $Ni(C_2H_4)$ in a triplet state, where the bonding is expected to be very weak [9]. The bond in the dimer complex is, however, considerably stronger and a larger distortion of ethene might have been expected. A possible explanation is the small basis set, especially the lack of diffuse $3d$-type functions on nickel, which results in an artificially large bond energy due to superposition error, but an inadequate description of the bonding.

The present study gives an ethene molecule, which is distorted 21% towards a single bonded ethane like structure.

Experimentally $Ni_x(C_2H_4)$ has been studied by Ozin et al. [2, 4] using matrix isolation techniques and infrared spectroscopy. They report $\nu_{CC} = 1488\ cm^{-1}$ in the nickel dimer complex as compared to $1623\ cm^{-1}$ for free ethene and $1499\ cm^{-1}$ for the monomer complex. These shifts agree well with the distortion found in the present work.

The nickel dimer can approach ethene in several symmetric geometric arrangements, of which the π-bonded end on structure (Fig. 1a) is the most likely to be bound [4, 5]. Arguments favoring this structure have been given previouly [4] including also a discussion of other possible structures of the complex (Fig. 1). These structures were scanned in search for local minima. No stable structures were, however, found which could be reached without passing a high energy barrier. A detailed investigation of the structure was therefore only performed for the end on complex.

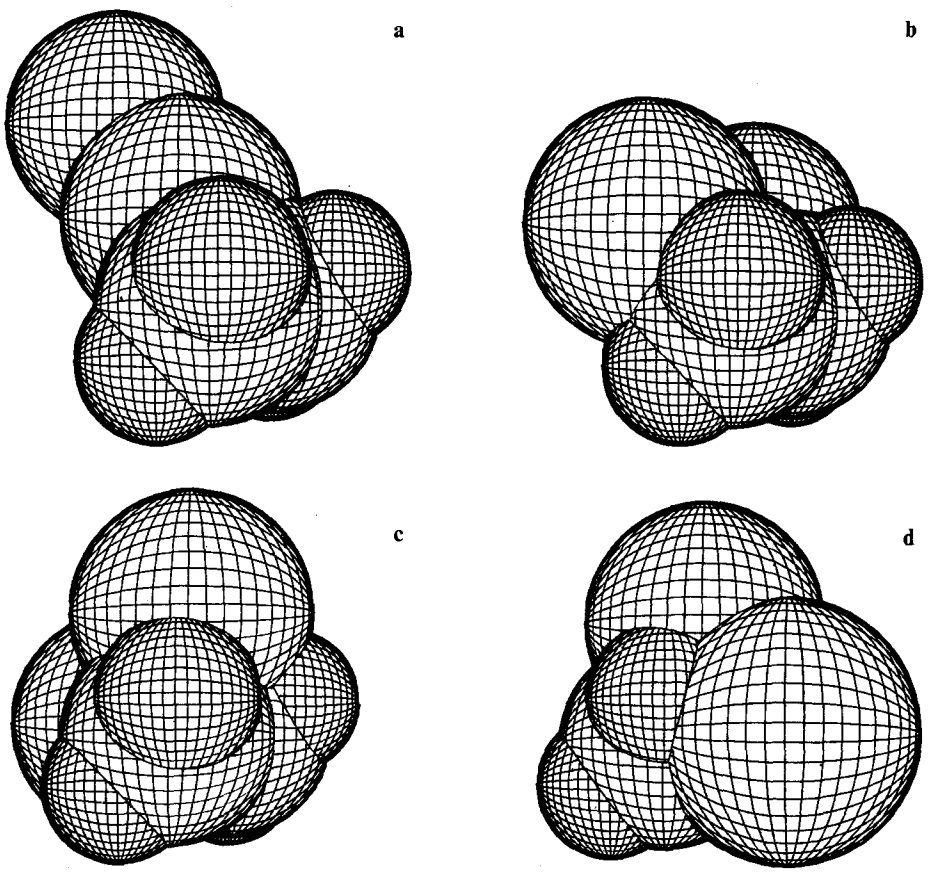

Fig. 1a–d. Considered geometry arrangements, with ethene fixed and Ni_2 in different positions. **a** End on; **b** parallel; **c** plane on perpendicular; **d** edge on perpendicular

The bonding 4s orbital ($4s_a + 4s_b$) is a diffuse doubly occupied orbital that will repell an approaching ethene if this repulsive overlap cannot be reduced somehow. Due to the mixing with $4p_z$ in forming the 4s bond, this repulsion is smallest if Ni_2 attach to ethene end on. The repulsion can be further reduced by polarizing the electrons to the nickel atom not facing ethene. In all three other cases (Fig. 1b-d), however, the repulsive overlap has to be reduced through a polarization perpendicular to the bond, a process implying a substantial lowering of the Ni-Ni bond by removing electron density from the bonding region.

2. Method

The basis set used for the nickel atom is the DZC-set of Tatewaki and Huzinaga [14], augmented with one diffuse s-type function (0.01474), two diffuse p-type functions taken from Roos and Veillard [15] and one diffuse d-type function (0.1650) yielding the contraction (3, 3, 3, 2, 1, 1*/3, 1*, 1*/3, 1, 1*) using the notation of Huzinaga et al. [16]. For carbon the MIDI-3 basis set of the same authors [17] was used, augmented with a polarizing d-type function (0.65) yielding the contraction (4, 2, 1/2, 1/1*). The basis set used for hydrogen is the 5s basis set of Huzinaga [18] contracted to 3s augmented with a polarizing p-type function (0.8) yielding (3, 1, 1/1*).

This basis set can be described as double-ζ plus polarization in the valence with a minimal basis set description of the core.

In all calculations the core orbitals, 1s, 2s, 3s, 2p, and 3p on nickel and 1s on carbon, were kept frozen in their atomic shape, $d^9s(^1D)$ for nickel and $s^2p^2(^3P)$ for carbon, to avoid superposition errors due to the relatively poor description of the core orbitals. Also all s-components of d-orbitals was deleted to make the analysis of the wavefunction easier.

The CASSCF method [19] used for the zeroth order wavefunction, is a special form of the MCSCF method where the orbital optimization is coupled with a full, symmetry and spin adapted, CI within a small orbital subspace, denoted the active space. The minimal active space to yield a qualitatively correct zeroth order wavefunction must include all orbitals with occupation numbers significantly differing from zero or two, especially those with occupation numbers changing with molecular geometry.

For $Ni_2(C_2H_4)$ in the end on structure (Fig. 1a) this is accomplished with the following active orbitals: Ni_2 has six almost degenerate spectroscopic states arising from two d^9s nickel atoms with a hole in the $3d\delta$ orbital. These states have the lowest energy of all possible d^9s states with $^3\Gamma_u$ as the ground state [20, 21]. The open shell orbitals are in the complex found in the representations a_1 and a_2 of the C_{2v} point group. At the asymptotic limit the choice is not important but at equilibrium the $d\delta$ orbitals in a_1 symmetry can mix with the $d\sigma$ orbitals due to the destruction of $D_{\infty h}$ symmetry. The CCπ will form a bonding orbital with a $4sp_z$ orbital at equilibrium and at the asymptotic limit the $\pi \rightarrow \pi^*$ excitations are

important. The d_{xz} orbital will donate electrons to CCπ*. Thus the active space should include the following orbitals

Orbital	Symmetry	Occupation
$Ni_A\ d\delta$	a_1	1
$Ni_B\ d\delta$	a_1	1
CCπ	a_1	2
CCπ*	b_2	0
$Ni_A\ d_{xz}$	b_2	2

This choice is confirmed by full valence CASSCF calculations, yielding no more important active orbitals. The CASSCF wave function will with the above active orbital space contain 28 symmetry adapted configuration state functions. The d-d holes can be coupled triplet or singlet with very small differences in energy. Many choices are therefore possible for the ground state electronic configuration. Since they are almost degenerate and show the same interaction with ethene, the specific choice is not important. The energy surface studied in the present work corresponds to the $^1A_1$ state of the complex.

On the top of the CASSCF calculations, contracted CI (CCI) [22] calculations were performed. All $3d$ electrons on the nickel facing the ethene, the $4s$ electrons, the CCσ and CCπ electrons were correlated. For technical reasons the singly occupied d orbital on the other nickel atom was also included, giving a total of 16 electrons. All configurations with a coefficient larger than 0.05 in the CASSCF wave function for any of the geometries considered were included in the reference space for the SD-CI wave function (cf Table 1).

This choice gave a total of 614217 singly and doubly excited CSF's which were then contracted to 1941 pair functions. The reader is referred to [22] for details about the contracted CI method. The geometry optimizations were performed both at the CASSCF and CCI levels of accuracy.

Table 1. Reference configurations in the contracted CI calculations

Ref	CCπ	$3d\delta$	$3d\delta$	$3d_{xz}$	CCπ*
Sym	a_1	a_1	a_1	b_2	b_2
1	2	2	0	2	0
2	2	0	2	2	0
3	2	2	0	0	2
4	2	0	2	0	2
5	2	2	0	1	1
6	2	0	2	1	1
7	2	1	1	1	1
8	0	2	0	2	2
9	0	0	2	2	2

3. Results

Four different geometric arrangements (Fig. 1) have been considered. Brief searches of minima was performed in all four cases, yielding only the end on case (Fig. 1a) as bound. The other arrangements were found to lead to repulsion between ethene and the nickel dimer. This does not mean that no other metastable conformations of the complex can be found, only that they cannot be reached without passing a high energy transition state. In the end on case, the repulsive overlap between the doubly occupied $4s$ orbital and the doubly occupied $CC\pi$ orbital can easily be reduced by pushing the $4s$ electrons to the nickel atom not facing ethene, and a bond can be formed between an empty $4sp_z$ and the $CC\pi$ orbital. When the nickel and carbon atoms get close and the $3d$ electrons get unshielded, the doubly occupied $3d_{xz}$ can form a bond with the empty $CC\pi^*$ orbital.

In the parallel case (Fig. 1b) the repulsive overlap must be reduced by polarizing the $4s$ electrons away perpendicular to the Ni-Ni bond, a procedure that is energetically unfavorable. Thus the $3d$ electrons are still shielded by the $4s$ electrons and no bonding occur. The same argument holds for the plane on perpendicular case.

In the edge on perpendicular case, there is the possiblilty of donating electrons from $CC\pi$ to $4s^*$, thus weakening both the NiNi and CC bonds. However no backdonation can take place, yielding a small effect. The nickel atoms get closer to the hydrogens than in the other cases leading to repulsive overlap between $4s$ and the hydrogens.

3.1. The end on structure

Geometry optimization was performed close to the energy minimum by computing a grid in two dimensions and performing polynomial fitting. The two parameters optimized are the nickel-carbon distance and a distortion parameter Q defined as follows. For $Q=0$ we have an undistorted ethene geometry and for $Q=1$ we have the ethane geometry with two hydrogens missing (cf Table 2).

The carbon-carbon distance and the two angles $\measuredangle$CCH and $\measuredangle$HCH were varied linearly with Q, but the carbon-hydrogen distance was kept fixed at 1.098 Å.

Table 2. Geometry of ethene as a function of the parameters Q and P

	$Q+P=0$	$Q+P=1$
R_{CC}	1.33 Å	1.53 Å
	$Q-P=0$	$Q-P=1$
$\measuredangle$HCH	117.8°	107.3°
$\measuredangle$CCH[a]	180.0°	231.7°

[a] The angle between the CC-axis and the bisector of the angle $\measuredangle$HCH

When the minimum for these two parameters was located, a third parameter, P, was introduced to allow stretching and bending optimize separately. The stretching and bending are varied linearly with P such that $Q+P$ describes the stretching and $Q-P$ describe the bending in such a way that $Q+P=0$ is no stretching and $Q+P=1$ is a carbon-carbon distance of ethane etc.

The Ni-Ni distance was kept fixed at 2.5 Å. It could be argued that the weakening of this bond due to the formation of a Ni-ethene bond would result in a longer Ni-Ni distance than in free Ni_2. This is most certainly the case, but the bond lengthening would be seriously overestimated at the level of theory used in the present work. CASSCF-CI calculations on the nickel dimer using basis sets of similar accuracy to those used here gives for the $^3\Gamma_u$ state a bond distance of 2.46 Å and a dissociation energy of 1.1 eV [21], which is only 46% of the experimental value (2.39 eV) [20, 23]. The difficulty in determining good dissociation energies for transition metal dimers is well known, and is due to large intra-atomic correlation effects which cannot properly be described using the conventional configuration interaction methods employed here. A free variation of the Ni-Ni distance would therefore lead to a too large weakening of the dimer bond. A compromise has been used, where the bond length is kept at a value slightly larger than it is in free Ni_2.

The geometry obtained at the CASSCF level is a nickel-carbon distance of 2.090 Å while the ethene is distorted 40% towards an ethane geometry, with no effect from the uncoupling of the stretching and bending distortion (cf Table 3). The bond energy was found to be only 4.1 kcal/mol.

At the CCI level the nickel-carbon distance increases by 0.049 Å to 2.139 Å while the ethene distortion decreases to 21%, with no effect from the uncoupling in this case either. The bond energy increases to 24.6 kcal/mol, which is further increased to 28.1 kcal/mol if the multireference analogue of the Davidson correction is included.

The binding mechanism can be described by a donation of electrons from $CC\pi$ to the empty $4sp_z$ hybrid pointing towards ethene and a backdonation from the doubly occupied $3d_{xz}$ to the empty $CC\pi^*$, as illustrated by the two molecular orbitals $17a_1$ and $8b_2$ in Figs. 2b and e.

Table 3. Geometry of $Ni_2(C_2H_4)$ in the $^1A_1$ state

	R_{NiC}	R_{CC}	∡HCH	∡CCH[c]	Q	P
CASSCF						
AL[a]	∞	1.354 Å	117.8°	180.0°	0.06	0.06
EQ[b]	2.090 Å	1.410 Å	113.6°	200.7°	0.40	0.00
CCI						
AL[a]	∞	1.342 Å	117.8°	180.0°	0.03	0.03
EQ[b]	2.139 Å	1.372 Å	115.6°	190.9°	0.21	0.00

[a] Asymptotic limit

[b] Equilibrium geometry

[c] The angle between the CC-axis and the bisector of the angle ∡HCH

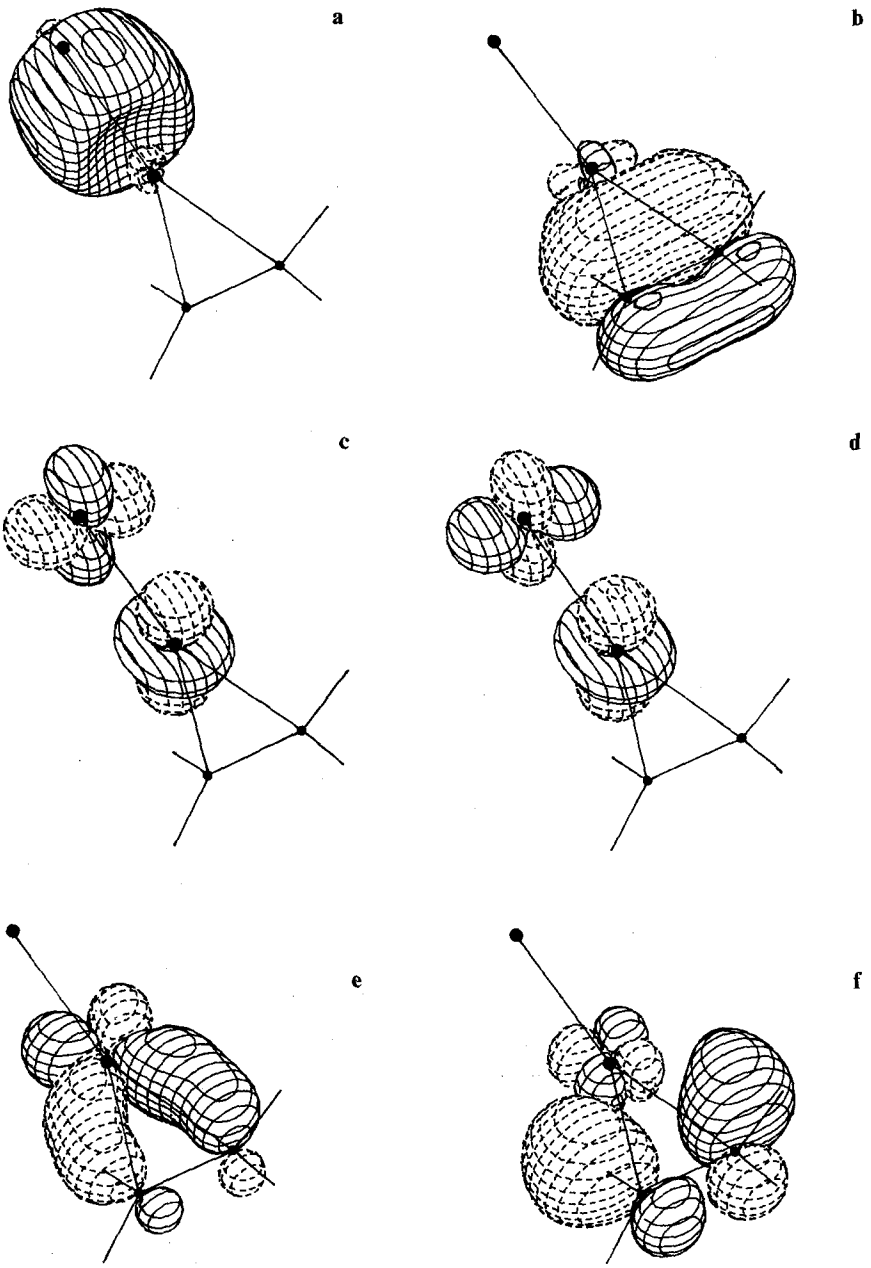

Fig. 2a–f. Natural orbitals at the CCI equilibrium geometry. **a** $16a_1$ $4s$; (occupation number: 2.00); **b** $17a_1$ CCπ (o.n.: 1.99); **c** $18a_1$ $3d$-hole (o.n.: 0.99); **d** $19a_1$ $3d$-hole (o.n.: 1.01); **e** $8b_2$ $3d_{xz}$ (o.n.: 1.82); **f** $9b_2$ CCπ^* (o.n.: 0.18)

This mechanism is enabled by pushing the $4s$ electrons to the nickel atom not facing ethene and thus unshielding the $3d$ orbitals (see orbital $16a_1$ in Fig. 2a).

The Mulliken population analysis results are presented in Table 4. Such a population analysis does not give a detailed picture of the charge flows in the system. It does, however, display the dominant features, especially if the charges are well localized. The main features of the bonding are also apparent from the charges. Thus the end nickel atom (Ni_B) has an excess $4s$ charge of 0.34 electrons and a total $3d$ population of close to nine electrons. The carbon bonded nickel (Ni_A) has on the other hand only 0.75 $4s$-electrons and 8.49 $3d$-electrons. The reduction in the $3d$ population is due to charge donation to the ethene moiety through the $3d_{xz}$ orbital.

At the CASSCF geometry the donation from $CC\pi$ to $4sp_z$, based on Mulliken population analysis, is 0.43 electrons while the backdonation from $3d_{xz}$ to $CC\pi^*$ is 0.57 electrons. At the CCI level these numbers drop to 0.37 and 0.47 respectively.

It is quite clear that the inclusion of dynamic correlation is of utmost importance for any quantitative results, both for the geometric structure and the bond energy, as has been noted in other work on transition metal compounds [24]. The

Table 4. Mulliken population analysis, at the CASSCF level, for $Ni_2(C_2H_4)$ at the CCI equilibrium geometry and the asymptotic limit

Occupations						
	Equilibrium			Asymptotic		
	Ni_A	Ni_B	C	Ni_A	Ni_B	C
s	0.75	1.34	1.21	0.95	0.95	1.18
p_z	0.25	0.07	1.03	0.06	0.06	0.98
$\Sigma\, d$[a]	3.01	2.98	—	2.99	2.99	—
p_x	0.06	0.00	0.94	0.00	0.00	0.94
d_{xz}	1.48	1.99	—	2.00	2.00	—
p_y	0.02	0.00	1.05	0.00	0.00	1.00
d_{yz}	2.00	1.99	—	2.00	2.00	—
d_{xy}	2.00	2.00	—	2.00	2.00	—
$\Sigma\, d$	8.49	8.96	0.05	8.99	8.99	0.05

Charges		
	Equilibrium	Asymptotic
$q(Ni_A)$	+0.43	0.00
$q(Ni_B)$	−0.37	0.00
q(C)	−0.29	−0.18
q(H)	+0.13	+0.09
$q(C_2H_4)$	−0.06	0.00
Donation:		
$d_{xz} \rightarrow CC\pi^*$	−0.47[b]	
$CC\pi \rightarrow 4sp$	−0.37[c]	

[a] Sum of all d-electrons in symmetry a_1

[b] Difference in occupation of $3d_{xz}$ and $4p_x$ at equilibrium and asymptotic limit

[c] Difference in occupation of $4s$ and $4p_z$ at equilibrium and asymptotic limit

somewhat paradoxical consequences on the bonding in the present system will be further elaborated in the discussion.

The superposition error was accounted for by allowing Ni_2 use the basis set of ethene, yielding an energy lowering of 0.25 kcal/mol, and by allowing ethene use the basis set of Ni_2, yielding an energy lowering of 2.58 kcal/mol, giving a total superposition error estimate of 2.83 kcal/mol.

4. Discussion

The Ni_2-C_2H_4 complex in the end on π-bonded configuration (Fig. 1a) exhibits large similarities with the Ni-C_2H_4 complex in the $^1A_1$ state [9]. In the monomer complex a nickel atom in the $d^9s(^1D)$ state interacts with an ethene. The major difference between these two systems lies in the $4s$ electrons. In the dimer case it can be pushed to the nickel atom not facing ethene while in the monomer case it has to remain on the nickel atom facing ethene. The way the monomer complex reduces the repulsive overlap is best described in the following way. The two open shells, $4s$ and $3d$, are coupled singlet, and this open shell configuration can equivalently be described by two closed shell configuration in the following way

$$c_1(4s+3d)^2-c_2(4s-3d)^2$$

with c_1 and c_2 equal. One of these sd hybrids point towards ethene and the other is perpendicular to the NiCC plane. When an ethene gets closer, c_1 and c_2 changes such that electrons migrate to the orbital perpendicular to the NiCC plane, and thus reduce the repulsive overlap. A more detailed discussion of this bonding mechanism can be found in [8] in which the constrained space orbital variation technique is used to analyse the bonding in some transition metal carbonyl complexes, including low spin NiCO. The geometry of the monomer complex is, at the CASSCF level, a nickel-carbon distance of 1.972 Å and an ethene distortion of 50% with a bond energy of 3.4 kcal/mol compared to 2.090 Å, 40% and 4.1 kcal/mol respectively for the dimer complex.

The back donation from $3d_{xz}$ to CCπ^* is 0.61 electrons for the monomer complex and 0.57 for the dimer complex, a small difference consistent with the bond length difference. The donation from CCπ to Ni, however, is quite different, 0.12 for the monomer complex and 0.43 for the dimer complex. This difference is due to the different role the $4s$ orbital plays in the two cases. In the monomer $4s$ forms a hybrid with $3d$, retaining its occupation number close to one, which does not increase the electron accepting power of the nickel atom. The polarization of the $4s\sigma$ orbital in Ni_2 on the other hand leads to a depopulated $4s$ orbital on the nickel atom facing the ethene carbons, which consequently becomes a good electron acceptor.

The above comparison between the monomer and dimer complex was made at the CASSCF level of approximation. Inclusion of dynamical correlation effects, however leads to a substantial change of the bonding properties. For the monomer complex these effects were only included at the equilibrium geometry determined by the CASSCF method. Thus the result reported in [9] do not reflect the

dynamical correlation effects on the geometry. Comparison with the present result shows that this leads to a too large distortion of the ethene geometry in the complex and a too short Ni–C distance. Even after correcting this error the monomer complex would most probably exhibit a slightly larger Ni–C distance and a longer CC bond than the dimer complex.

The effects of the dynamical correlation on the dimer complex is somewhat puzzling. The Ni–C distance becomes 0.05 Å longer, but the bond energy increases from 4 to 25 kcal/mol. At the same time the CC bond length decreases from 1.41 to 1.37 Å, while the decrease is only 0.01 Å for free ethene (cf Table 3). The smaller distortion of the ethene molecule is not difficult to understand. Both the bonding and anti-bonding π-orbitals were active in the CASSCF calculations. Such an active space leads to an overestimation of the anti-bonding effect and consequently to a too long and too weak CC bond. This effect is further enhanced when electrons are donated into the anti-bonding π-orbital. Dynamical correlation decreases this effect and leads therefore to stronger and shorter bonds. The result is a smaller charge transfer from nickel to carbon (*vide infra*), and a longer nickel-carbon bond. One would then expect also the bond strength to decrease. This is, however, counterbalanced by the strengthening of the bond resulting from the inclusion of dynamical correlation into the $3d$ electrons on the bonded nickel atom, which is known to lead to a substantial increase in the bond energy.

The effect can be described by a simple electrostatic model. Dynamic correlation increases the force constant for the distortion of ethene, thus reducing the distortion and the induced dipole moment. Therefore the Ni–C bond strength is reduced while the bond distance is increased. This decrease is more than compensated for by a dispersion interaction due to large polarizability of both ethene and the nickel dimer.

Ozin et al. [4] have performed GVB-CI calculations on the end on π-bonded Ni_2–C_2H_4 complex in the $^3A_2$ state. The basis set used was an effective core potential with double-ζ description of $4s$, single-ζ description of $3d$ plus a polarizing $4p$ on nickel. The ethylene basis set was of double-ζ quality. The bond energy obtained is 27.2 kcal/mol with a nickel-carbon distance of 2.07 Å, and a virtually undistorted ethene moiety. The binding picture is rather inaccurate despite a bond energy close to what is found in the present work. The $4s$ is pushed to the nickel atom not facing ethene, as in the present work. The minimal basis description of the $3d$ orbitals does not allow the $3d_{xz}$ back donation to CCπ^* which is the major part of the binding. On the other hand it also yields a superposition error of the order of 15 kcal/mol, estimated as the difference between the bond energies found for the monomer complex in [4] and [9], respectively. The two effect apparently cancels to a large part.

The result of the matrix isolation infrared spectroscopy measurements of Ozine et al. which can most easily be compared to the present theoretical predictions is the shift of the CC stretch frequency. The value for free ethene is 1623 cm^{-1} [25]. For the monomer complex they obtain the value 1499 cm^{-1}, a shift of 124 cm^{-1}. A slightly larger shift (135 cm^{-1}) is obtained for the dimer complex.

The corresponding frequency for ethane is 945 cm^{-1}. Assuming a similar bond strength one would for the hypothetical singly bonded bi-radical CH_2-CH_2 obtain a frequency close to 1000 cm^{-1}. The estimated total shift from a double bond is then around 600 cm^{-1}. It is probably slightly smaller, since the presence of the nickel-carbon bonds increases the value of the CC force constant. The measured frequency shifts are for the monomer and dimer complex respectively around 21 and 22% of the total shift expected for a complete annihilation of the double bond in ethene. These values are consistent with the result obtained here for the dimer complex. The calculated change in the geometry of ethene in the complex is 21% towards an ethane like structure. A sightly smaller value is expected for the monomer complex as deduced from a comparison of the CASSCF results. From the CASSCF results obtained in our previous study of the monomer complex it was concluded that the singlet ground state was probably not formed in the low temperature matrix, since a barrier exists between this state and the asymptotic triplet ground state, which has a height of approximately 10 kcal/mol. This conclusion was based on the too large geometry change found for the singlet ground state on the CASSCF level of the theory. In light of the present results this conclusion must be revised. If dynamical correlation effects are included in the geometry determination a modification of around 20% towards a single bonded ethane like ligand would most probably be obtained in good agreement with the frequency shifts reported by Ozin et al. [2, 4]. This discussion is obviously oversimplified, since it does not include the coupling between the different vibrational modes.

5. Conclusions

The results of this work conclusively shows that the nickel dimer forms an end-on π-bonded complex with ethene. There are no other bound configurations, except for the possibility of some meta-stable cases. This is a consequence of the repulsive overlap between the sigma bond in the Ni_2 species with the CCπ or the hydrogens in these arrangements.

Dynamic correlation has a profound effect on both the binding energy and the geometry of the complex (the latter at variance with systems like NiCO [7]). Dynamic correlation increases the force constant of ethene, reducing the distortion and the induced dipole moment of ethene, yielding a weaker Ni-C bond and longer bond distance. This decrease in binding energy is more than compensated for by a dispersion interaction due to large polarizability of both ethene and the nickel dimer.

The results of the present work also gives new insight of the Ni-C_2H_4 complex, and the conclusions reached in our previous work [9] have to be modified.

References

1. Heck RF (1974) Organotransition metal chemistry, a mechanistic approach. Academic Press, New York, p 84; Mango FD (1975) Coord Chem Rev 15:109; Khan MMT, Martell AE (1974) Homogeneous catalysis by metal complexes, vol 2. Academic Press, New York, p 77; Jolly PW,

Wilke G (1974) The organic chemistry of nickel, vol 1 (organonickel compounds) Academic Press, New York
2. Ozin GA (1979) Coord Chem Rev 28:117
3. Geusic ME, Morse MD, Smalley RE (1985) J Chem Phys. 82:590
4. Ozin GA, Power WJ, Upton TH, Goddard III WA (1978) J Am Chem Soc 100:4750; Upton TH, Goddard III WA (1978) J Am Chem Soc 100:321
5. Basch H, Newton MD (1977) J Chem Phys 69:584
6. Rives AB, Fenske RF (1981) J Chem Phys 75:1293
7. Blomberg MRA, Brandemark UB, Siegbahn PEM, Broch-Mathisen K, Karlström G (1985) J Chem Phys 89:2171
8. Bauschlicher Jr CW, Bagus PS, Nelin CJ, Roos BO (1986) J Chem Phys 85:354
9. Widmark P-O, Roos BO, Siegbahn PEM (1985) J Phys Chem 89:2180
10. Widmark P-O, Sexton GJ, Roos BO (1986) Theochem 135:235
11. Blomberg MRA, Siegbahn PEM (1983) J Chem Phys 78:986; J Chem Phys (1983) 78:5682
12. Siegbahn PEM, Blomberg MRA, Bauschlicher Jr CW (1984) J Chem Phys 81:2103
13. Rösch N, Rhodin TN (1974) Faraday Discuss Chem Soc 58:28
14. Tatewaki H, Huzinaga S (1979) J Chem Phys 71:4339
15. Roos BO, Veillard A, Vinot G (1971) Theor Chim Acta 20:1
16. Huzinaga S (1984) Gaussian basis sets for molecular calculations. Elsevier, Amsterdam
17. Tatewaki H, Huzinaga S (1980) J Comput Chem 1:205
18. Huzinaga S (1965) J Chem Phys 42:1293
19. Roos, BO, Taylor PR, Siegbahn PEM (1980) Chem Phys 48:157; Roos BO (1980) Int J Quantum Chem S14:175; Siegbahn PEM, Almlöf J, Heiberg A, Roos BO (1981) J Chem Phys 74:2384
20. Noell JO, Newton MD, Hay PJ, Martin RL, Bobrowitcz FW (1980) J Chem Phys 73:2360
21. Nelin CJ, Roos BO, unpublished results
22. Siegbahn PEM (1981) In: Carbo R (ed) Current aspects of quantum chemistry. Proceedings of the International Congress, Barcelona, Spain, 1981. Elsevier, Amsterdam, 1981
23. Kant A (1964) J Chem Phys 41:1872
24. Bauschlicher Jr CW, Walch SP, Langhoff SR, J Chem Phys, in press
25. Hertzberg G (1966) Molecular spectra and molecular structure. III. Electronic spectra and electronic structure of polyatomic molecules. Van Nostrand, New York